MOLECULAR AND CELLULAR BIOLOGY, June 1993, p. 3359–3369
0270-7306/93/063359-11$02.00/0

Vol. 13, No. 6

Sequences within the Last Intron Function in RNA 3′-End Formation in Cultured Cells

DOBRILA NESIC,† JIU CHENG, AND LYNNE E. MAQUAT*

Department of Human Genetics, Roswell Park Cancer Institute, Buffalo, New York 14263

Received 28 December 1992/Returned for modification 2 February 1993/Accepted 16 March 1993

In cultured cells, little if any mRNA accumulates from an intronless version of the human gene for triosephosphate isomerase (TPI), a gene that normally contains six introns. By deleting introns either individually or in combinations, it was demonstrated by Northern (RNA) blot hybridization that while the deletion of a greater number of introns generally results in a lower level of product mRNA, not all introns contribute equally to mRNA formation. For example, intron 1 appeared to be dispensable, at least when the remaining introns are present, but deletion of the last intron, intron 6, reduced the level of product mRNA to 51% of normal. To determine how intron 6 contributes to mRNA formation, partial deletions of intron 6 were constructed and analyzed. Deletion of the lariat and acceptor splice sites or the donor, lariat, and acceptor splice sites, each of which precluded removal of the intron 6 sequences that remained, reduced the level of product mRNA to <1 or 27% of normal, respectively. As measured by RNase mapping and cDNA sequencing, the decrease in mRNA abundance that was attributable to the complete and partial intron 6 deletions was accompanied by an increase in the abundance of pre-mRNA that lacked a mature 3′ end, i.e., that was neither cleaved nor polyadenylated. We infer from these and other data that sequences within the final intron facilitate proper 3′-end formation, possibly through an association with the components of a productive spliceosome.

Genomic constructs of protein-encoding genes are often expressed more efficiently than their intronless counterparts. In some cases, this is attributable to the presence within one or more introns of enhancers or other *cis*-acting elements that influence transcription initiation or elongation (24, 34). In other cases, introns may contain sequences that influence nucleosome composition and/or binding so as to augment the accessibility of chromosome domains to transcription or elongation factors (47). Additionally, introns may generally facilitate aspects of nuclear RNA processing, nuclear RNA stability, and/or mRNA transport to the cytoplasm, possibly as a function of a productive association with spliceosomes and other ribonucleoprotein particles and the consequential metabolic events that include but are not limited to splicing (14).

Evidence exists that the abnormally low level of mRNA that derives from many (5–7, 12, 17, 19–21, 40, 43) but not all (2, 35, 48) intron-containing genes when they are expressed in intron-free form is the result of inefficiencies in RNA processing. These inefficiencies manifest as a decrease in RNA stability in the nucleus and an impairment in RNA export to the cytoplasm (28, 43). Considering introns individually and disregarding the special cases of alternative RNA splicing (29, 32, 45), the role of the final intron in posttranscriptional RNA processing is best understood. Niwa et al. (39) have demonstrated for a chimeric RNA containing a single adenovirus intron upstream of the late simian virus 40 (SV40) polyadenylation signal that in nuclear extracts polyadenylation precedes splicing in an intron-dependent manner. The intron sequences that function in polyadenylation were found to comprise the splice acceptor site but not the splice donor site (39). Essentially the same conclusion was reached by Alwine and coworkers (11) when transfecting COS cells with constructs that consisted of the chloramphenicol acetyltransferase (CAT) gene flanked by the SV40 late gene promoter-leader and polyadenylation signals. The results of both studies were interpreted to indicate that definition of the 5′ end of the final exon by spliceosome assembly at the acceptor site of the upstream intron accelerates the rate of RNA 3′ end formation, i.e., endonucleolytic cleavage and, subsequently, polyadenylation. This interpretation is consistent with the finding, by transient cell transfection, that the presence of an intron within an RNA targets that RNA toward the polyadenylation pathway (23, 41). In fact, the presence of an intron can influence the way in which at least one nuclear factor associates with the RNA sequences that direct polyadenylation. This was evident with the demonstration that cross-linking of the heterogeneous nuclear ribonucleoprotein C polypeptide to RNA sequences within the SV40 late polyadenylation site is altered by the insertion of an intron, although the functional significance of the alteration is not understood (46). Conversely, mutation of the AAUAAA polyadenylation signal has been shown by using nuclear extracts to depress splicing of the final intron but not the penultimate intron (37). Somewhat at odds with the data that functionally link the final intron to the process of 3′-end formation was the finding that the same chimeric RNA that was used in the Niwa et al. (39) study could be cleaved and polyadenylated after it had been spliced, provided that it was first extracted from agarose and deproteinized (36). The kinetics of cleavage and polyadenylation were similar to those for the unspliced species and, therefore, contraindicated a role of the final intron in 3′-end formation. We rationalized that studies using intact cells so that all cellular factors would be present at physiological concentrations should help to resolve the function of the final intron in 3′-end formation. If a function were indicated, then it would also be possible to localize the relevant intron sequences by deletion analysis.

In this report, we begin to examine in cultured cells the

* Corresponding author.
† Permanent address: Institute for Nuclear Sciences-Vinca, Belgrade, Yugoslavia.

role of introns on the posttranscriptional processes of RNA that encodes the glycolytic enzyme triosephosphate isomerase (TPI). We have found that processing of the transcripts that derive from the transient expression of a human TPI gene in mouse L cells is qualitatively and quantitatively similar to the processing of transcripts that derive from the endogenous TPI gene of a human melanoma cell line. Thus, transient transfection should provide a biologically sound means to determine the effects of specific mutations within the TPI gene on the metabolism of bona fide TPI RNA. By transient transfection, the effect on mRNA production of deleting introns individually and in combinations has been quantitated by Northern (RNA) blot analysis. Additionally, the functional interplay between splice sites within the final intron (intron 6) and efficient 3'-end formation has been examined by RNase mapping and cDNA sequencing. While many laboratories have shown that splicing and polyadenylation can proceed independently in vitro (for a review, see references 27 and 51), our data are consistent with the idea (11, 23, 37–39, 41, 49) that the two reactions are coupled by the process of spliceosome assembly on the last intron.

MATERIALS AND METHODS

Cell culture. The human melanoma cell line Malme-3 was grown in RPMI 1640 medium containing 10% bovine calf serum. Mouse Ltk$^-$ cells were grown in minimal essential medium containing 10% fetal calf serum and 5% bovine calf serum.

Construction of pMT-TPI DNAs that lack one or more TPI gene introns. pMT-TPI Δ(introns 2-6) was created by the trimolecular ligation of the 1.3-kbp *Nco*I-*Fsp*I fragment that spans exon 1 through exon 2 of the TPI gene, the 527-bp *Fsp*I-*Eco*RI fragment that spans exon 2 through exon 7 of TPI cDNA, and the 3.4-kbp *Eco*RI-*Nco*I fragment that consists of the distal end of exon 7 of the TPI gene, all of pUC13, the MT-1 promoter, and the proximal end of exon 1 of the TPI gene. The proximal end of exon 7 plus 1.1 kbp of 3'-flanking sequences were then inserted at the *Eco*RI site as a 1.6-kbp *Eco*RI fragment.

pMT-TPI Δ(introns 3-6) was created by the bimolecular ligation of the 5.8-kbp *Bcl*I-*Bcl*I fragment that consists of the distal end of exon 7 of the TPI gene, all of pUC13, exon 1 through exon 3 of the TPI gene, and the 1.14-kbp *Bcl*I-*Bcl*I fragment that spans exon 3 through exon 7 of TPI cDNA.

pMT-TPI Δ(intron 1) was created by the trimolecular ligation of the 190-bp *Nco*I-*Fsp*I fragment that spans exon 1 through exon 2 of TPI cDNA, the 1.4-kbp *Fsp*I-*Eco*RI fragment that spans exon 2 through exon 7 of the TPI gene, and the 3.4-kbp *Eco*RI-*Nco*I fragment. The 1.6-kbp *Eco*RI fragment was then inserted at the *Eco*RI site.

pMT-TPI Δ(introns 1,6) was created by the trimolecular ligation of the 190-bp *Nco*I-*Fsp*I fragment of TPI cDNA, the 1.3-kbp *Fsp*I-*Eco*RI fragment that was isolated from pMT-TPI Δ(intron 6) (10) and spans exon 2 through exon 7, and the 3.4-kbp *Eco*RI-*Nco*I fragment. The 1.6-kbp *Eco*RI fragment was then inserted at the *Eco*RI site.

pMT-TPI Δ(introns 2,6) was created by the trimolecular ligation of the 1.38-kbp *Nco*I-*Bcl*I fragment that was isolated from pMT-TPI Δ(introns 2-6) and spans exon 1 through exon 3, the 1.1-kbp *Bcl*I-*Eco*RI fragment that was isolated from pMT-TPI Δ(introns 1-5) and spans exon 3 through exon 7, and the 3.4-kbp *Eco*RI-*Nco*I fragment. The 1.6-kbp *Eco*RI fragment was then inserted at the *Eco*RI site.

pMT-TPI Δ(intron 2) was created by the trimolecular ligation of the 1.38-kbp *Nco*I-*Bcl*I fragment that was isolated from pMT-TPI Δ(introns 2-5) and spans exon 1 through exon 3, the 1.24-kbp *Bcl*I-*Eco*RI fragment that spans exon 3 through exon 7 of the TPI gene, and the 3.4-kbp *Eco*RI-*Nco*I fragment. The 1.6-kbp *Eco*RI fragment was then inserted at the *Eco*RI site.

pMT-TPI Δ(introns 1-6) was created from pMT-TPI by replacing the 3.1-kbp *Nco*I-*Nco*I fragment that spans exon 1 through exon 7 with the corresponding 1.1-kbp *Nco*I-*Nco*I fragment of TPI cDNA (30).

Construction of pMT-TPI DNAs that contain partial deletions of intron 6. A 34-bp deletion of the lariat and acceptor sites (Δ 5' TCTTGACCAAGCCCTTGTTCTGCTCCCTTCC CAG 3' of the sense strand) within TPI gene intron 6 was introduced into subclones of the 660-bp *Pst*I-*Eco*RI fragment from pMT-TPI^{norm} (10) by using the mutagenic oligonucleotide 5' CCCAGTCACAGAGCΔATGGGATGAGTCTGCC 3' and the method of Kunkel et al. (26) as previously described (10). A 6-bp deletion of the donor site (Δ 5' GTGAGT 3' of the sense strand) of this intron was then introduced by using the mutagenic oligonucleotide 5' CCGG GAACCAAAGCCΔCTCCATAAATGA 3'. All mutagenized fragments were sequenced in their entirety before being used to reconstruct pMT-TPI plasmids (13). Subsequent to reconstruction, the *Hgi*AI site in exon 6 of each of these constructs was treated with Klenow to generate a 4-bp deletion which restored the site of translation termination to normal.

Construction of pSPTPI templates. Derivatives of the TPI gene were constructed in pSP65 in order to provide DNA templates for the synthesis of nonradioactive TPI RNAs with SP6 RNA polymerase (Promega). To construct pSPTPI/c, the 110-bp *Bss*HII-*Sac*I fragment of the TPI gene that extends from 1 bp upstream of the transcription initiation site to the middle of exon 1 was inserted into pSD3 (a gift from P. Good and J. Mertz). Prior to insertion, pSD3 was cleaved with *Eco*RI and *Sac*I, and both insert and vector were made blunt with Klenow. Next, the 1,120-bp *Sac*I-*Pst*I fragment of TPI cDNA (30) was inserted into the *Sac*I and *Pst*I sites of M13mp18. This fragment extends from exon 1 up to and including the $(A \cdot T)_{14}$ $(C \cdot G)_{15}$ sequence residing immediately downstream of the final exon. By oligonucleotide-directed mutagenesis, the $(A \cdot T)_{14}$ $(C \cdot G)_{15}$ region was specifically deleted. pSPTPI/c was then generated by inserting the resulting *Sac*I-*Pst*I fragment of TPI cDNA into the *Sac*I and *Sma*I sites of the above-described derivative of pSD3. Prior to insertion, the 3' overhang of the *Pst*I site was removed with Klenow. For RNA synthesis, pSPTPI/c was linearized immediately downstream of the tract of 60 to 80 A · T bp with *Hin*dIII. The synthesized RNA differs from bone fide TPI mRNA in having an additional 12 nucleotides (nt) at the 5' end and an additional 7 nt immediately upstream of the poly(A) tract. pSPTPI/c+3' was constructed by replacing the 735-bp *Nde*I-*Hin*dIII fragment of pSPTPI/c, which includes the last 365 bp of exon 7 and 3'-flanking sequences including the A · T base pair tract, with the 642-bp *Nde*I-*Pvu*II fragment of the TPI gene, which includes the last 365 bp of exon 7 and 277 bp of 3' flanking DNA. Prior to in vitro RNA synthesis, pSPTPI/c+3' was linearized with *Pvu*II. RNA synthesized from pSPTPI/c+3' was identical to RNA synthesized from pSPTPI/c, except that the poly(A) tract and the 7 nt immediately upstream of the tract were replaced by the 277 nt that normally reside downstream of the TPI gene.

Cell transfections and RNA purifications. Test plasmids were derivatives of pMT-TPI in which the mouse MT-1 promoter including 6 bp of adjacent 5' untranslated region was inserted 1 bp upstream of the transcription initiation site

of the complete TPI gene with a synthetic *Bam*HI linker (13). The reference plasmid, pMT-Gl, harbored a hybrid human-mouse β-globin gene that, like the TPI gene in the pMT-TPI constructs, was driven by the MT-1 promoter (10). Mouse Ltk$^-$ cells were transfected at 60 to 80% confluency with DEAE-dextran and a 3.15 M excess of a pMT-TPI test plasmid relative to the pMT-Gl reference plasmid (a total of 24 μg/15-cm dish unless otherwise specified) basically as described previously (10), except that 5% bovine calf serum was substituted for 5% Nuserum. Total, nuclear, and cytoplasmic RNAs were isolated 36 h after transfection (13). Poly(A)$^+$ and poly(A)$^-$ RNAs were isolated by two passages through a column of oligo(dT)-cellulose (1).

RNA blot analysis. Total RNA (25 μg) was denatured with glyoxal, electrophoresed in a 1.5% agarose gel (33), and transferred to a nylon membrane (Zeta-bind). Blot hybridization was performed with two DNA fragments that had been ^{32}P labeled by random priming (16). MT-TPI RNA was detected with a 300-bp *Nco*I-*Nde*I fragment that derived from the 3' untranslated region of human TPI cDNA. MT-Gl RNA was detected with a 170-bp *Bal*I-*Dra*I fragment that derived from exon 3 of the mouse β^{major}-globin gene. Hybridization and washing conditions were such that human but not mouse TPI RNA was detected (10).

RNA probe synthesis and RNase mapping. A fragment of the TPI gene and mouse β^{major}-globin cDNA were inserted, respectively, into pGEM3Z and pGEM4Z DNAs (Promega) downstream of and in opposite orientation to the T7 promoter in order to serve as templates for the synthesis of ^{32}P-labeled antisense RNA. The 642-bp *Nde*I-*Pvu*II of the TPI gene, which includes 365 bp of the 3' untranslated region and 277 bp of 3'-flanking DNA, was used to map the cleavage and polyadenylation sites of TPI RNA. The 235-bp *Bam*HI-*Mbo*II fragment from mouse β^{major}-globin cDNA, which includes 19 bp of exon 2 and 216 bp of exon 3, was used to control for experimental variations. The pGEM3Z/TPI construct was linearized with *Hin*dIII, and the pGEM4Z/Gl construct was linearized with *Eco*RI, and each linearized product was transcribed in vitro with T7 polymerase (Promega) and [α-^{32}P]GTP (Amersham). The resulting transcripts were mixed in hybridization buffer (Ambion) with either L-cell RNA, Malme-3 cell RNA, or sense RNA that had been synthesized in vitro from one of the pSPTPI constructs or the pGEM4Z/Gl construct with SP6 polymerase. After denaturation, the hybridization temperature was allowed to drop from 85 to 55°C over a period of 12 to 16 h. Hybrids were exposed to RNase A and RNase T_1 (Ambion) for 30 min at 37°C, concentrated by precipitation, denatured, and electrophoresed in an 8.3 M urea–5% polyacrylamide gel. Quantitative analysis was performed with a PhosphorImager (Molecular Dynamics).

The polymerase chain reaction (PCR) and analysis. cDNA was synthesized from 0.8 to 1.5 μg of poly(A)$^+$ RNA with the mouse mammary leukemia virus reverse transcriptase (Superscript, GIBCO-BRL) and 100 pmol of the primer P2 (5' CCCAAGCTTGTTTTTTTTTTTT 3'). The 3' end of P2 is complementary to poly(A) and harbors a *Hin*dIII site surrounded by sequences that ensure efficient cleavage by the enzyme when in the context of double-stranded DNA. Amplification was then carried out with *Taq* polymerase (Perkin-Elmer Cetus), an additional 100 pmol of P2, and 100 pmol of P1 (5' GATGGCTGCAGTCCAACGTCTC 3'), which harbors a *Pst*I site. After 25 amplification cycles, reaction products were gel purified, digested with *Pst*I and *Hin*dIII, gel purified again, and inserted into M13mp18 DNA. Recombinant single-stranded M13 DNAs were sequenced by dideoxy chain termination. The universal primer was used to obtain the sequence that resided upstream of the poly(A) tract. The primer P3 (5' ATTCGGGCTTGAGGGA AG 3'), which is perfectly complementary to exon 7 of TPI cDNA, was used reconfirm the intron 6 sequence.

RESULTS

The introns in MT-TPI pre-mRNA are not functionally equivalent. In previous studies, sequences specific to TPI gene introns were not found to influence TPI promoter function (4). In these studies, the level of mRNA that was produced as a result of transcription initiation from a 2,800-bp promoter fragment of the human TPI gene was comparable regardless of whether the TPI gene, including all of its six introns, or the human β-globin gene, including both of its two introns, had been placed downstream. The level of mRNA that was produced by analogous constructs in which transcription initiated from a 595-bp promoter fragment of the TPI gene (4) was also comparable, albeit slightly (1.3-fold) lower than when the 2,800-bp promoter fragment directed transcription. However, TPI gene introns do appear to influence posttranscriptional RNA processes, since the level of mRNA that was produced by a construct that harbored TPI cDNA in the place of the TPI gene was barely detectable (see below).

To examine further the posttranscriptional contribution of TPI introns to gene expression, TPI gene variants that precisely lacked one or more introns were constructed with pMT-TPI, a plasmid that harbored a normal TPI gene that was driven by the mouse (m) metallothionein (MT)-1 promoter rather than the TPI promoter (10, 13) (Fig. 1). Each variant was transiently expressed in mouse L cells together with a reference plasmid, pMT-Gl, in which a hybrid human-mouse β-globin gene was likewise driven by the mMT-1 promoter (10). The reference plasmid served to control for variations in transfection efficiency and RNA recovery. After transfection, total L-cell RNA was isolated, and MT-TPI and MT-Gl gene expression was quantitated by Northern blot hybridization (Fig. 2).

Each of the intronless variants that was tested produced an abnormally low level of mRNA with the exception of Δ(intron 1), the variant that lacked only intron 1 (Fig. 1 and 2; see Fig. 4, lane 4). Intron 1 also appeared to be dispensable when analyzed in *cis* with the deletion of intron 6 [compare Δ(intron 6) to Δ(introns 1,6)]. By itself, intron 1 was ineffective in producing a significant level of mRNA. In contrast to the deletion of intron 1, the deletion of intron 2 or intron 6 reduced the mRNA level to 17 and 51% of normal, respectively. In *cis*, the effects of the intron 2 and 6 deletions were cumulative. One or a combination of introns 3 through 5 also contributed to mRNA production, as evident from the very low level (≤12% of normal) of mRNA produced by Δ(introns 3-6), Δ(introns 2-6), and the completely intronless variant, Δ(introns 1-6). The results of nuclear run-on analyses indicated that none of the introns significantly increase the rate of transcription initiation (unpublished data). The level of MT-TPI gene transcription was not altered by the deletion of introns 3 through 6 and was reduced no more than twofold by the deletion of all introns. Therefore, some of the introns must contribute to the posttranscriptional processing of MT-TPI RNA, and the degree of contribution is not the same for all introns. Furthermore, splicing per se is not sufficient for the efficient production of MT-TPI mRNA. None of the intron deletions created an internal exon that is larger than 300 nt, the maximum length that is believed to be

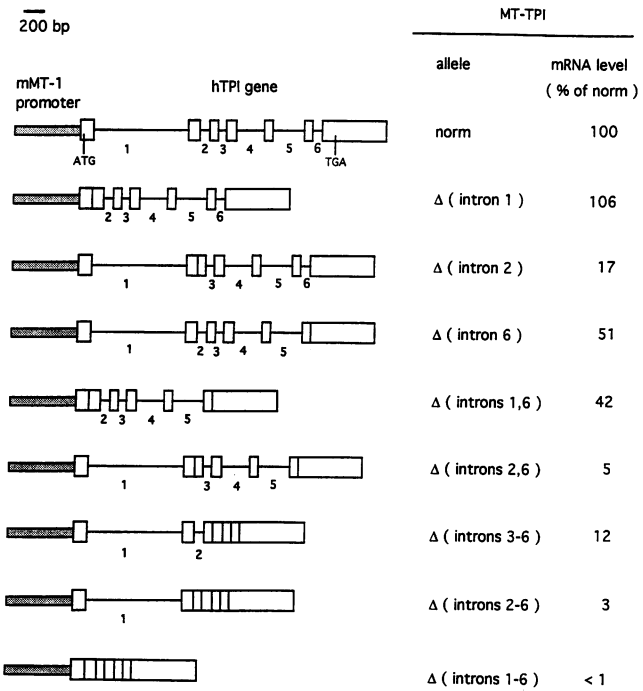

FIG. 1. Structures of the MT-TPI alleles in the pMT-TPI constructs that lack one or more TPI gene introns. The stippled bar represents the 750-bp *Bam*HI-*Bam*HI fragment that harbors the mMT-1 promoter. Boxes and interspersed lines designate, respectively, the exons and introns of the human (h) TPI gene. The introns are numbered. Not shown are the 1.1 kbp of human DNA that resides downstream of the TPI gene and that is present in each plasmid construct. ATG and TGA designate the translation initiation and termination codons, respectively. The percentage of MT-TPI^{norm} mRNA (norm) was calculated by Northern blot hybridization (Fig. 2) and represents the average of three independently performed experiments.

allowable without causing difficulties in exon definition and spliceosome assembly (22, 42). Thus, the reduced level of mRNA that is characteristic of the intronless variants should not be attributable to inefficient or inaccurate splicing because of the creation of an excessively large exon. Consistent with this, none of the intronless variants produced a detectable level of abnormally sized mRNAs.

Sequences within intron 6 influence the efficiency of mRNA production. In order to begin to understand the role of individual introns in the production of MT-TPI mRNA, the effects of two deletions within intron 6 were examined in the presence of all other introns. The first deletion, Δ(lar-acc), removed the distal-most 34 bp of the intron that comprise the lariat and acceptor splice sites; the second deletion, Δ(don/lar-acc), removed an additional 6 bp at the extreme proximal end of the intron that comprise the donor splice site (Fig. 3). Initially, the effects of each deletion on MT-TPI mRNA abundance and size were analyzed by Northern blot hybridization (Fig. 4). TPI mRNA of the human melanoma cell line Malme-3 was analyzed in parallel. The deletion Δ(lar-acc) reduced the level of MT-TPI mRNA so that it was barely detectable, whereas the deletion Δ(don/lar-acc) reduced the level of mRNA, on average, to 27% of normal. Each of these partial intron 6 deletions was more deleterious to gene expression than was Δ(intron 6), the complete intron 6 deletion, which reduced the level of mRNA, on average, to 51% of normal.

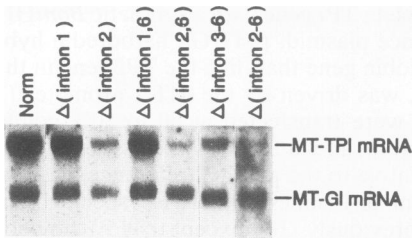

FIG. 2. Analysis by Northern blot hybridization of the pMT-TPI intronless variants. Mouse L cells (3×10^7/15 cm) were cotransfected with 12 μg of the specified pMT-TPI construct and 12 μg of pMT-Gl DNA. Total cellular RNA (25 μg) from the transfected L cells was denatured, electrophoresed in agarose, transferred to a nylon membrane, and cohybridized with the ^{32}P-labeled 300-bp *Nde*I-*Nco*I fragment of TPI cDNA and the ^{32}P-labeled 170-bp *Bal*I-*Dra*I fragment of the mouse β^{major}-globin gene. The level of each MT-TPI mRNA was normalized to the level of MT-Gl mRNA and then calculated as a percentage of MT-TPI^{norm} mRNA. In each experiment, the percentage of MT-TPI^{norm} mRNA was defined as 100. The data for Δ(intron 6) are shown in Fig. 4, lane 4. The data for Δ(introns 1-6) are not shown.

In order to determine if the slightly larger-than-normal size of the mRNA produced by the Δ(don/lar-acc) variant corresponded to intron 6 sequences that remained unprocessed, as was expected, and in order to assess the exon 6-exon 7 junction within the mRNAs produced by the remaining three constructs, cDNA of MT-TPI RNA was synthesized with RNA from each of the L-cell transfections. The cDNA was amplified by the polymerase chain reaction (PCR), and individual amplification products were cloned and sequenced from the distal end of exon 6 to the proximal end of exon 7. Results indicated that RNA produced by the Δ(lar-acc) construct was, indeed, present and contained the remaining 94 nt of intron 6. Also as expected, mRNA produced by the Δ(don/lar-acc) construct contained the remaining 88 nt of intron 6, and mRNA that derived from the Δ(intron 6) construct completely lacked intron 6 sequences and harbored exon 6 precisely juxtaposed to exon 7 (data not shown). Thus, none of these deletions resulted in the use of cryptic splice sites within either of the flanking exons. Furthermore, the size of each product mRNA that was detected by Northern blot hybridization (Fig. 4) was consistent with the sequence data, suggesting that none of the

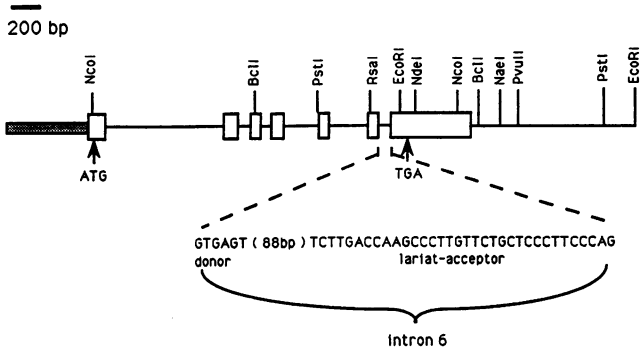

FIG. 3. Structure of the MT-TPI gene and the intron 6 deletions. The sequences deleted at the donor and lariat-acceptor sites of intron 6, the last intron, are specified below the diagram of the gene, to either side of the remaining 88 bp of the intron. Not all cleavage sites within the TPI gene for the enzymes *Rsa*I and *Pvu*II are shown.

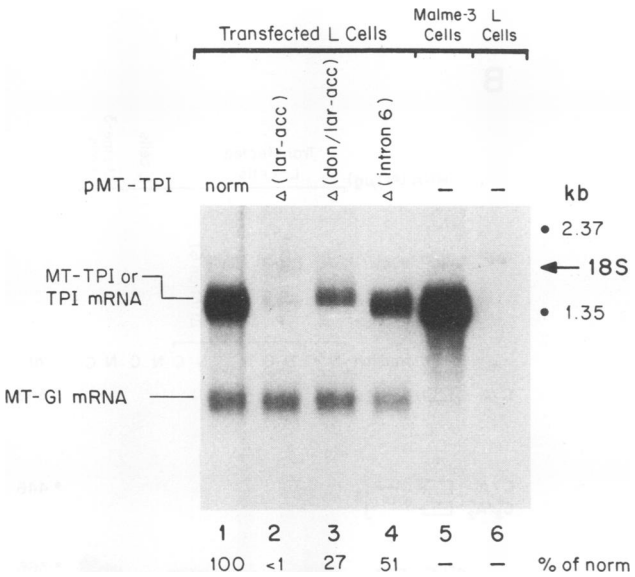

FIG. 4. Analysis by Northern blot hybridization of the effects of the intron 6 deletions on the abundance of MT-TPI mRNA. Mouse L cells were cotransfected with 12 μg of the specified pMT-TPI construct and 6 μg of pMT-GI DNA. Total cellular RNA (25 μg) from the transfected L cells and, as controls, untransfected mouse L cells and human Malme-3 cells was analyzed as described in the legend to Fig. 2. MT-TPI mRNA varies in size as a consequence of the intron 6 sequences that remain unprocessed. The positions of the 2.37- and 1.35-kb molecular size standards are provided. The percentages of MT-TPI^{norm} (% of norm) represent the average of four independently performed experiments.

intron 6 deletions qualitatively altered the removal of another intron.

Incidentally, the mRNAs produced by the Δ(don/lar-acc) and Δ(lar-acc) constructs prematurely terminate translation because of nonsense codons that reside within the unprocessed intron 6 sequences. However, the altered translational state of the mRNAs was shown not to contribute to the reduction in mRNA abundance by deleting 4 nt within exon 6. The deletion restored the translational reading frame of each mRNA to normal but did not affect the mRNA level (data not shown). This result was expected, given that nonsense codons downstream of the middle of exon 6 do not affect the abundance of MT-TPI mRNA (10).

Sequences within intron 6 influence the efficiency of 3'-end formation. Experiments were designed to correlate the level of MT-TPI mRNA that derived from each of the four MT-TPI constructs with the efficiency of proper 3'-end formation. Proper 3'-end formation was analyzed with RNase mapping to localize the 3' termini of the transcripts in total or nuclear and cytoplasmic fractions of transfected L cells. The probe consisted of a uniformly ^{32}P-labeled, antisense transcript of 699 nt, 642 of which consisted of TPI gene sequences that included 365 nt of the 3' untranslated region and 277 nt of 3'-flanking DNA (Fig. 5C). RNase mapping was made quantitative by concomitantly assaying for RNA that derived from the reference pMT-GI construct with another uniformly ^{32}P-labeled, antisense transcript of 298 nt, 235 of which consisted of mouse β^{major}-globin cDNA that included 19 nt of exon 2 and 216 nt of exon 3 (Fig. 5C).

The MT-TPI RNA produced in L cells by the normal construct, like the endogenous TPI RNA produced in human Malme-3 cells, protected several regions of the TPI probe from digestion. For total, nuclear, and cytoplasmic RNA, the most abundant of these regions migrated broadly at 365 nt (Fig. 5A, lanes 1 and 6; Fig. 5B, lanes 1, 2, 11, and 12). Analysis of both MT-TPI mRNA and the TPI mRNA of Malme-3 cells by PCR amplifying, cloning, and sequencing individual cDNAs of each mRNA (see below) indicated that the breadth of the protected fragments reflects mostly incomplete cleavage of the probe by RNases A and T_1 rather than a significant amount of heterogeneity at the 3' termini. In fact, protection of a single 365-nt portion of the probe was predicted on the basis of previous sequence analyses of TPI cDNA clones that derived from adult liver (30). Thus, the protected fragments that migrated at or around 365 nt were likely the result of hybridization to both MT-TPI and TPI mRNAs that terminated at the most frequently used cleavage and polyadenylation site, which will be referred to as pA. Consistent with this interpretation, RNA that was synthesized in vitro from an intronless TPI DNA template (pSPTPI/c) and that terminated with a synthetic tract of poly(A) at the pA site protected the same fragments (Fig. 5A, lane 7).

Other nuclease-resistant regions of the TPI probe that were protected by transcripts from both the normal MT-TPI allele as well as the TPI gene of Malme-3 cells consisted of approximately 642 and 446 nt. The 642-nt fragment, which was detected with total and nuclear but not cytoplasmic RNA, derived from hybridization of the probe to transcripts having 3' ends that extended beyond the limits of the probe and into a region that is devoid of a pA signal as determined by DNA sequencing of 850 bp beyond the probe (34a). The 446-nt fragment, which was detected with total, nuclear, and cytoplasmic RNA, could derive from hybridization of the probe to transcripts having 3' ends that arose by use of what appears to be a reasonably good alternative pA signal (50, 52) that will be referred to as the pA2 site. Additionally, the 446-nt fragment could derive from hybridization to the same transcripts that protected the 642-nt fragment, provided that the resulting hybrids were subsequently cleaved by RNases within or around the stretch of 13 A · U base pairs that resides 83 nt downstream of the pA site. Actually, both possibilities appear to be realized. In support of the first possibility, there exists a putative pA signal (UAUAAA) together with a suitably spaced cleavage and polyadenylation site (C↓A) and a suitably spaced GU box (GGUU UN_{21}UUUUU) that, if used, would generate an RNA that protects 446 nt of the probe. Furthermore, cleavage and polyadenylation appear to be a prerequisite for RNA export to the cytoplasm (15), and a fraction of the RNAs having 3' ends that map to this site are found in the cytoplasm (see below). In support of the second possibility, RNA that was synthesized in vitro from an intronless TPI DNA that terminated at the *Pvu*II site residing 277 nt downstream of the TPI gene (pSPTPI/c+3') and included the internal oligo(A) tract also gave rise to the 446-nt fragment when analyzed by RNase mapping (Fig. 5A, lane 8). Furthermore, the abundance of the 446-nt fragment and, by inference, the frequency of cleavage by RNases A and T_1 was found to increase with a temperature-induced increase in breathing at the A · U duplex (data not shown). For the purposes of discussion, the RNA that protects the 642-nt portion of the probe will be referred to as C^-/A^- (for not cleaved and not polyadenylated), the RNA that protects the 446-nt portion of the probe will be referred to as a mixture of C^-/A^- and C_2^+/A_2^+ (for cleaved and polyadenylated at the pA2 site), and the RNA that protects the 365-nt portion of the probe will be referred to as C^+/A^+. Notably, the RNA that protects

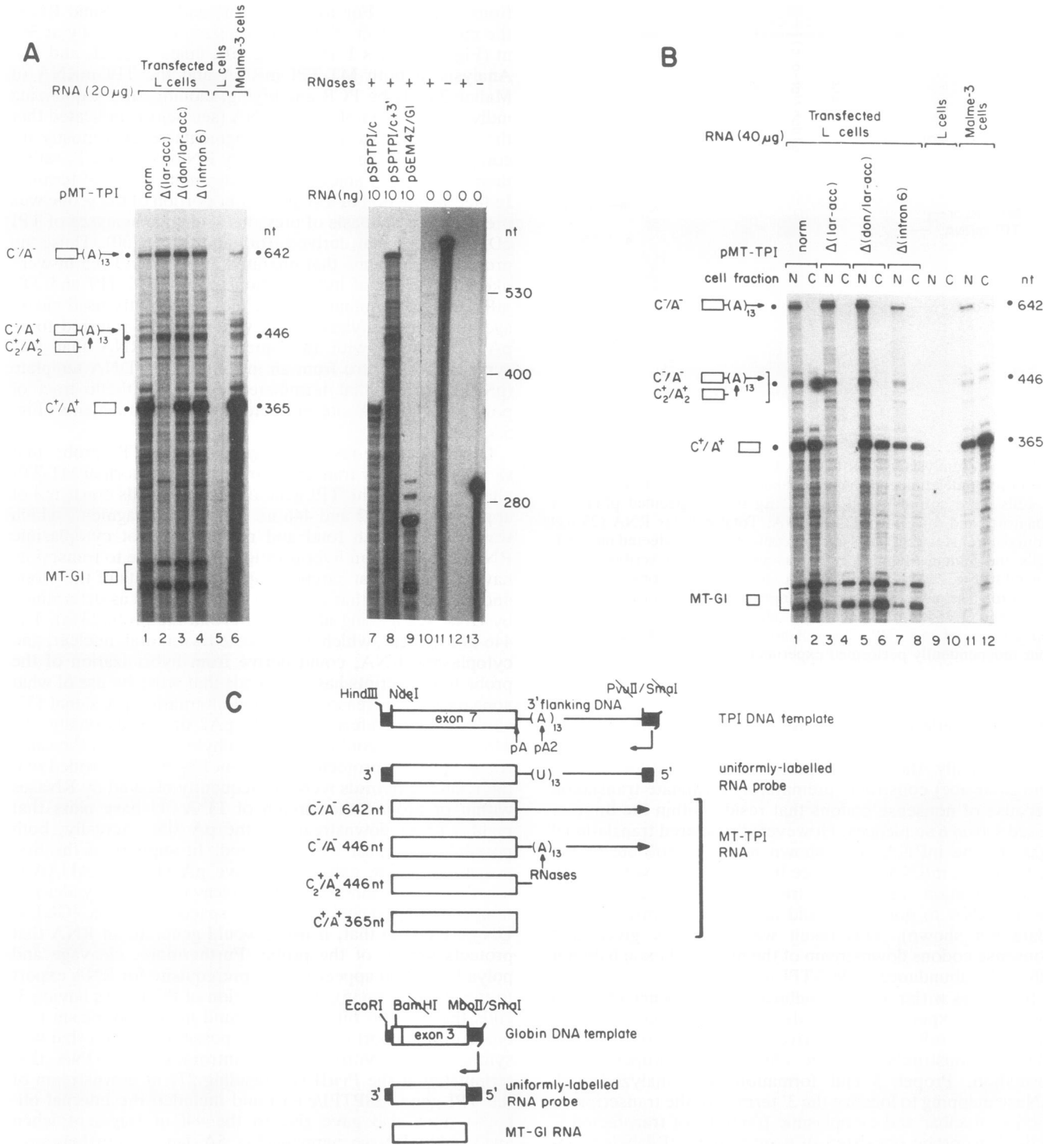

FIG. 5. Analysis by RNase mapping of the effects of the intron 6 deletions on 3′-end formation. Total cell RNA (A) or nuclear (N) and cytoplasmic (C) cell RNA (B) were isolated from L cells (cotransfected as described in Materials and Methods), Malme-3 cells, and untransfected L cells. RNA that was synthesized in vitro was also analyzed in parallel (A). This RNA derived from pSPTPI/c, which generates intronless TPI RNA that terminates with a synthetic tract of poly(A) at the pA site; pSPTPI/c+3′, which generates intronless TPI RNA that terminates at the *Pvu*II site residing 277 nt downstream of the pA site; or GEM4Z/GI, which contains 9 nt of exon 2, 216 nt of exon 3, and 39 bp of the pGEM4Z polylinker sequence. Analysis consisted of hybridization with probes for both TPI and β-globin RNAs. A 642-nt TPI probe was synthesized from recombinant pGEM3Z that contains human TPI DNA from the *Nde*I site in exon 7 to the *Pvu*II site in 3′-flanking DNA. A 298-nt globin probe was synthesized from recombinant pGEM4Z that contains mouse β^{major}-globin cDNA from the *Bam*HI site in exon 2 to the *Mbo*II site in exon 3. Prior to electrophoresis, samples were treated with a mixture of RNases A and T_1. As a control, 1/10 of each of the input RNA probes was electrophoresed without exposure to RNases in lanes 11 and 13 (A). C^+/A^+ specifies the 365-nt region of the TPI probe that was protected by TPI transcripts that had been cleaved and polyadenylated at the pA site. The 642- and 446-nt regions of the TPI probe were protected by C^-/A^- transcripts that were apparently neither cleaved nor polyadenylated, i.e., extended beyond the *Pvu*II site

TABLE 1. TPI RNA levels[a]

TPI RNA	Total cell RNA				Nuclear RNA				C^+/A^+ cytoplasmic RNA (% of norm)
	% of (C^-/A^- + C^+/A^+)		% of norm		% of (C^-/A^- + C^+/A^+)		% of norm		
	C^-/A^-	C^+/A^+	C^-/A^-	C^+/A^+	C^-/A^-	C^+/A^+	C^-/A^-	C^+/A^+	
MT-TPI									
norm	8	92	100	100	20 ± 4	80 ± 4	100	100	100
Δ(lar-acc)	85	15	206	3.3	77	23	370 ± 20	18 ± 2	0.3 ± 0
Δ(don/lar-acc)	23	77	170	53	39 ± 1	61 ± 1	240 ± 14	61 ± 4	43 ± 1
Δ(intron 6)	17	83	140	68	33 ± 1	67 ± 1	168 ± 33	69 ± 6	65 ± 8
TPI of Malme-3 cells	12	88			15 ± 3	85 ± 3			

[a] The level of each MT-TPI RNA and the TPI RNA of Malme-3 cells was quantitated by phosphorimaging. The phosphorimaging intensity of each RNase-resistant portion of the probe was normalized by correcting for the number of radioactive nucleotides. The level of each MT-TPI RNA was additionally normalized to the level of MT-Gl mRNA in order to control for variations in the efficiencies of transfection, cell fractionation and RNA recovery. In determining the percentage of (C^-/A^- plus C^+/A^+), the sum of the normalized values for the C^-/A^- (i.e., 642- and 446-nt fragments) and C^+/A^+ species that derive from each MT-TPI construct or the TPI gene of Malme-3 cells was defined as 100%. In determining the percentage of the norm, the normalized values for the C^-/A^- or C^+/A^+ transcripts were calculated as a percentage of the normalized values, respectively, for the C^-/A^- or C^+/A^+ transcripts that derived from the normal MT-TPI construct, each of which was defined as 100. The numbers represent the average of at least two independently performed experiments.

642 nt is likely to be C^-/A^-, since it is not detected in the cytoplasm and lacks a canonical pA signal downstream of the pA2 site. However, this possibility is not proven. The 642-nt protected fragment does not derive from hybridization of the probe to transfecting DNA, since the quantity of the protected fragment is not affected by pretreating the RNA with RQ RNase-free DNase (Promega) (data not shown). We believe that the RNA that protects the 446-nt fragment consists mostly of C^-/A^- RNA, considering that it manifests an abundance paralleling the abundance of the RNA that protects the 642-nt fragment (Fig. 5) and considering that the pA2 site is inefficiently used relative to the pA site. A small fraction of this RNA from both the normal MT-TPI construct and the TPI gene of Malme-3 cells was detected in the cytoplasm (Fig. 5B, lanes 2 and 12) and may represent C_2^+/A_2^+ transcripts. As expected, the C^+/A^+ transcripts from both of these genes is the major RNA species that was detected in the cytoplasmic fraction (Fig. 5B, lanes 2 and 12).

In the case of the Δ(lar-acc) construct, deletion of the lariat and acceptor sites within intron 6 reduced the level of C^+/A^+ transcripts in total, nuclear, and cytoplasmic RNA to 3.3, 18, and 0.3% of the normal level, respectively (Fig. 5A, lane 2; Fig. 5B, lanes 3 and 4; Table 1). The ability to detect C^+/A^+ RNA in total RNA by RNase mapping but not Northern blot hybridization (Fig. 4, lane 2) reflects the relative sensitivity of the two assays. Concomitant with the decrease in C^+/A^+ transcripts, C^-/A^- transcripts in total and nuclear RNA were increased to 206 and 370% of the normal level, respectively (Fig. 5A, lane 2; Fig. 5B, lane 3; Table 1). The finding that C^+/A^+ transcripts were undetectable in the cytoplasmic fraction (Fig. 5B, lane 4; data not shown for Northern blotting) is in keeping with the notion that spliceosome assembly, in this case presumably at the donor site of intron 6, can impair RNA export to the cytoplasm when not removed by the process of splicing (8, 18, 25, 28, 43). However, the possibility that the RNA is exported from the nucleus and subsequently degraded in the cytoplasm cannot, a priori, be discounted. These data indicate that the reduced level of C^+/A^+ transcripts in both the nucleus and the cytoplasm is likely to be the result of inefficient 3'-end formation due to the Δ(lar-acc) deletion and are consistent with the demonstration with nuclear extracts that a single base change within the acceptor site of the intron that precedes the poly(A) site affects the efficiency of cleavage and polyadenylation (39). In theory, the reduced level of the C^+/A^+ transcripts could also be attributable to an abnormally increased rate of decay of these transcripts in the nucleus.

In the case of the Δ(don/lar-acc) construct, the additional deletion of the donor site of intron 6 restored the efficiency of proper 3'-end formation to closer to normal. The levels of C^+/A^+ transcripts in total, nuclear, and cytoplasmic RNA were 53, 61, and 43% of normal, respectively (Fig. 5A, lane 3, Fig. 5B, lanes 5 and 6; Table 1), and was accompanied by an increase in the level of C^-/A^- transcripts in both total and nuclear RNA to 170 and 240% of normal, respectively, (Fig. 5A, lane 3; Fig. 5B, lane 5; Table 1). Since the level of C^+/A^+ RNA in the nucleus was 61% of normal and the level in the cytoplasm was 70% the level in the nucleus (i.e., 43% of normal), this RNA may manifest a below-normal half-life in the nucleus, a below-normal efficiency of export to the cytoplasm, a below-normal half-life in the cytoplasm, or any combination of these possibilities. Regardless, the reduced level of C^+/A^+ RNA in both the nucleus and the cytoplasm is at least partly due to inefficient 3'-end formation. Export of this species would be predicted from the finding that the residual 88 nt of intron 6 are no longer recognized as excisable sequences and, instead, become part of the final exon as discussed above.

In the case of the Δ(intron 6) construct, the deletion of all of intron 6 was even more effective in restoring the efficiency

of the probe and, in the case of those that protected the 446-nt region, were cleaved by RNases A and T_1. The 446-nt region also was protected by C_2^+/A_2^+ transcripts that were cleaved and polyadenylated at the pA2 site. The C_2^+/A_2^+ transcripts in panel B, lane 2, are partly obscured by a spot of radioactivity; however, the transcripts do exist, as was evident in two other independently performed experiments. Two regions of the globin probe that consisted of 235 and 250 nt were protected by MT-Gl transcripts, as confirmed by using only the globin probe and the RNA that was analyzed in panel A, lane 2 (data not shown). As an additional confirmation, the same two regions were protected by transcripts that derived from L cells that had been transfected solely with pMT-Gl. The probes and the protected fragments are diagrammed(C). Diagonal lines through a restriction enzyme indicate the destruction of the enzyme cleavage site during the cloning process.

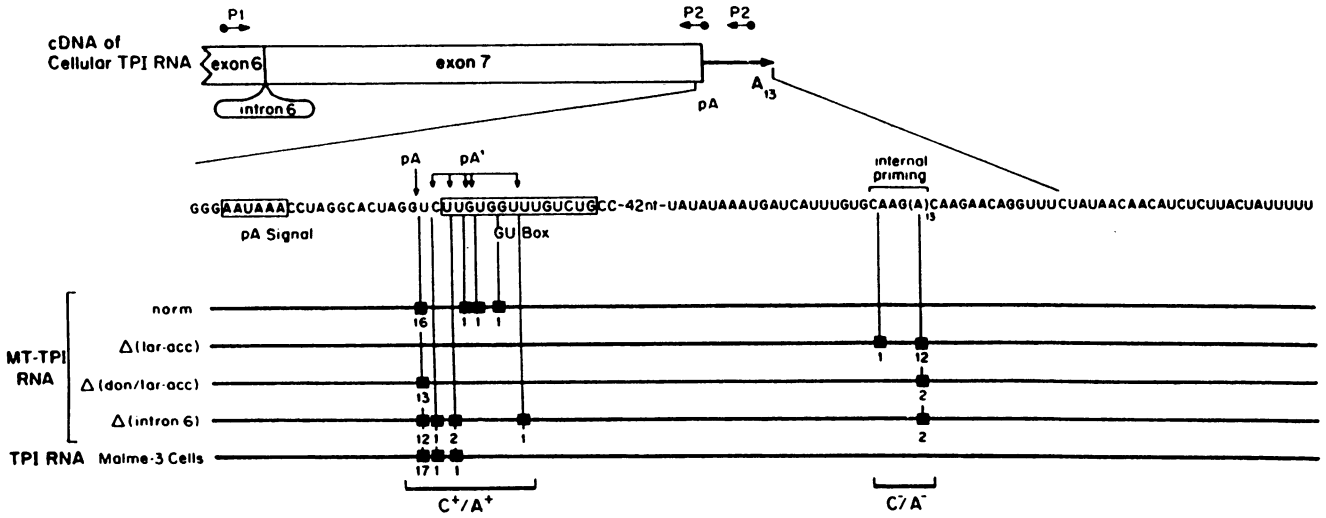

FIG. 6. PCR analysis of the effects of the intron 6 deletions on 3'-end formation. cDNA was made with the primer P2 and poly(A)$^+$ RNA that derived from the L-cell transfectants or, as a control, Malme-3 cells. The cDNA was then amplified with the primers P1 and P2. The positions of primer annealing are designated with the dots specifying primer 5' ends and the horizontal arrows specifying the directions of primer extensions. The multiple positions of P2 annealing correspond to the poly(A) tract that is added posttranscriptionally at the pA and pA' sites and the oligo(A)$_{13}$ tract that resides 83 nt downstream of pA. A partial sequence of exon 7 and 3'-flanking DNA is shown below the cDNA. Within this sequence, the pA signal and G/U box are boxed, and vertical arrows specify the pA and pA' sites. For each RNA specified, vertical lines mark the 3' termini of the PCR products and numbers denote the number of PCR products having each terminus. C$^+$/A$^+$, cleaved and polyadenylated; C$^-$/A$^-$, neither cleaved nor polyadenylated. Incidentally, the 3'-most sequences include the relatively infrequently used pA2 site and the GU box of which consists of GGUUUN$_{21}$UUUUU.

of proper 3'-end formation to normal. The level of C$^+$/A$^+$ transcripts from this construct in total, nuclear, and cytoplasmic RNA was 68, 69, and 65% of normal, respectively (Fig. 5A, lane 4; Fig. 5B, lanes 7 and 8; Table 1), and the level of C$^-$/A$^-$ transcripts was increased in total and nuclear RNA to only 140 and 168% of the normal level, respectively (Fig. 5A, lane 4; Fig. 5B, lane 7; Table 1). While this increase is undoubtedly responsible for the decrease in the level of both nuclear and cytoplasmic C$^+$/A$^+$ RNA, it is also possible that C$^+$/A$^+$ RNA is degraded at an abnormally increased rate in the nucleus. Since the level of this RNA was comparable in both the nucleus and the cytoplasm, this RNA was exported to the cytoplasm with a normal efficiency where it manifested a normal half-life.

It can be concluded by consolidating the data from Northern blotting (Fig. 4) and RNase mapping (Fig. 5) that each of the intron 6 deletions reduces the level of MT-TPI mRNA. The concomitant accumulation of C$^-$/A$^-$ RNA suggests that the reduction is due, at least in part, to the inefficient formation of proper 3' ends. The reason for the variable levels of C$^-$/A$^-$ transcripts that are evident for a particular construct when comparing total and nuclear RNA fractions, albeit from different transfections, is unknown. Possibly, the variable levels reflect differences in the metabolic state of posttransfection cells. Regardless, in all instances, a lower level of C$^+$/A$^+$ RNA was accompanied by a higher level of C$^-$/A$^-$ RNA, and the level of C$^-$/A$^-$ RNA that derived from each of the constructs, irrespective of the transfection, was always Δ(lar-acc) > Δ(don/lar-acc) > Δ(intron 6) > normal.

The TPI pA site is the predominant but not sole site of cleavage and poly(A) addition. Next, the precise sites of cleavage and polyadenylation that characterize the TPI transcripts of Malme-3 cells and the MT-TPI transcripts of each L-cell transfectant were localized. To this end, cDNA was synthesized from the poly(A)$^+$ fraction of total cell RNA with the primer P2 [5' CCCAAGCTTG(T)$_{12}$ 3']. Because this primer primes both the poly(A) tract that is added posttranscriptionally and the oligo(A) tract that resides downstream of the site of poly(A) addition, the relative abundance of C$^+$/A$^+$ and C$^-$/A$^-$ transcripts can be used as an additional measure of the efficiency of 3'-end formation, providing that the priming efficiencies of the two tracts are equal. The cDNAs were amplified by PCR with, as primers, P2 and P1 (5' GATGGCTGCAGTCCAACGTCTC 3'), the latter of which primes within exon 6 (Fig. 6), and individual PCR products were cloned and sequenced.

Only PCR products that corresponded to C$^+$/A$^+$ transcripts were obtained for normal MT-TPI RNA and the TPI RNA of Malme-3 cells (Fig. 6). While the pA site was used 87% of the time, additional sites of cleavage and polyadenylation were evident. These sites resided downstream of the pA site, within the GU box, and they have been designated pA' (Fig. 6). Thus, 3'-end formation at the pA site is usually but not always confined to a single nucleotide. This may reflect that, despite the presence of a consensus pA signal and GU box in TPI RNA, the G ↓ U pA site deviates from the more commonly used C ↓ A or U ↓ A pA sites (3, 50) (Fig. 6). This idea is consistent with the finding with nuclear extracts that mutation of the consensus C ↓ A pA site to a nonconsensus C ↓ C or C ↓ U pA site results in heterogeneity in the site of cleavage without an effect on the efficiency of 3'-end formation (44).

Deletion of the lariat and acceptor sites precluded the detectable production of C$^+$/A$^+$ RNA. All of the 13 Δ(lar-acc) transcripts that were analyzed were C$^-$/A$^-$, as indicated by all of the corresponding PCR products having a distal end that coincided with the internal oligo(A) tract. These findings are not unexpected, given the low level of C$^+$/A$^+$ RNA that was characteristic of the Δ(lar-acc) construct. Also following expectations, transcripts that derived from both the Δ(don/lar-acc) and Δ(intron 6) constructs were primarily (87 and 89%, respectively) C$^+$/A$^+$ but also C$^-$/A$^-$

(13 and 11%, respectively). As for the normal MT-TPI construct, heterogeneity at the site of cleavage and poly(A) addition was evident for Δ(intron 6). A complete sequence analysis of each of the PCR products (data not shown) demonstrated that the intron 6 sequences were present or absent from the product mRNA of each construct as demonstrated previously by PCR analysis of the RNAs examined by Northern blotting (Fig. 4). It should be noted that a significantly larger number of PCR products would have to be analyzed in order to detect the relatively infrequently used pA2 site.

DISCUSSION

In this report, we examine in cultured cells the role of introns within TPI pre-mRNA. We have found that not all introns contribute equally to mRNA formation. Of the individual introns examined, intron 1 appears to be dispensable. In contrast, introns 2 and 6 are less dispensable. While the role of intron 2 remains to be addressed, intron 6 appears to function in 3'-end formation. It does not appear to function in transcription initiation as demonstrated by nuclear run-on analysis of intron 6-less and intron 6-containing constructs (unpublished data). Deletion of the lariat and acceptor sites of this intron resulted in an abnormally high nuclear level of nonadenylated transcripts having a 3' end that extended beyond the most frequently used site of cleavage and poly(A) addition and essentially eliminated mRNA formation. At face value, these findings suggest that 3'-end formation is negatively affected by either the failure to assemble components of a spliceosome at the lariat-acceptor splice site or the partial assembly of a spliceosome (i.e., at the donor but not lariat-acceptor splice site). Data from other laboratories demonstrating that deletion of the donor site of the last intron has little or no effect on 3'-end formation (11, 39) support the first possibility (see below). Therefore, the lariat-acceptor splice site of the final intron appears to function in 3'-end formation. However, the second possibility is also realistic, given recent studies of adenovirus constructs harboring a polyadenylation signal downstream of an exon into which a donor splice site had been inserted (38). As a consequence of the insertion, product RNA was inefficiently polyadenylated and inefficiently cross-linked to the CstF polyadenylation factor in nuclear extracts. In an analogous fashion, it is possible that spliceosome assembly at the intron 6 donor site of Δ(lar-acc) transcripts inhibits 3'-end formation by inhibiting the lariat-acceptor splice site of the penultimate intron, intron 5, from substituting for the lariat-acceptor splice site that was deleted from intron 6. A direct test for function of the intron 6 donor splice site on 3'-end formation proved to be uninformative, since deletion solely of this site resulted in exon 6 skipping (unpublished data). This result is not unexpected for an RNA harboring multiple introns (9, 42 and references therein).

The requirement of a functional splice acceptor site within the last intron for efficient 3'-end formation is consistent with data that derive from cultured cells for either SV40-CAT gene transcripts (11) or SV40 late gene transcripts (49) and data that derive from nuclear extracts for transcripts of an adenovirus-SV40 gene under some (39) but not all (36) circumstances. The SV40-CAT gene transcripts harbored two SV40 donor sites upstream of a single SV40 acceptor site. The adenovirus-SV40 gene transcripts contained two exons and a single intron of the major late transcription unit of human adenovirus fused within exon 2 to a polyadenylation cassette from the late unit of SV40. In contrast to deleting the acceptor site, deleting either the 3'-most donor site of the SV40-CAT gene (11) or the only donor site of the adenovirus-SV40 gene was found to have no effect on the efficiency of 3'-end formation, suggesting that it is spliceosome assembly at the acceptor site rather than the process of intron removal per se that facilitates 3'-end formation. It was hypothesized that spliceosome assembly at the acceptor site of the last intron may facilitate the binding of the complex that is active in pre-mRNA cleavage and polyadenylation (39). Our data validate this hypothesis.

The finding that the Δ(lar-acc) transcripts, unlike those that harbor a normal intron 6 sequence, are not detected in the cytoplasm corroborates the observation (8, 28, 43) that spliceosome assembly on an RNA precludes the export of that RNA to the cytoplasm. We reason that spliceosome assembly at the intron 6 donor site in the absence of spliceosome assembly at the intron 6 lariat-acceptor site results in nuclear retention either directly, or because of the negative effect on RNA 3'-end formation, or both. Consistent with these reasonings, the additional deletion of this donor site alleviates, albeit incompletely, both the block in RNA export and the inefficiency in RNA 3'-end formation.

The construct in which all of intron 6 is deleted resulted in a lower level of RNA with an unprocessed 3' end and a higher level of mRNA (51% of normal) than either the Δ(lar-acc) or the Δ(don/lar-acc) construct. The conclusion that intron 6 augments 3'-end formation derives solely from these findings. A similar conclusion was reached for the human β-globin gene. Complete deletion of the final (second) intron of the globin gene was found to reduce the level of β-globin mRNA by reducing the efficiency of 3'-end formation, while deletion of the first intron was found to have a less drastic effect on the level of mRNA without an effect on 3'-end formation (12). For the TPI gene, the fact that some properly cleaved and polyadenylated RNA is formed in the absence of intron 6 suggests that one or more of the remaining introns can serve as a functional substitute for intron 6 with about half the efficiency. It is possible that the reduction in mRNA abundance that accompanies the sole deletion of intron 2 as well as the deletions of more than one intron (Fig. 1 and 2) is due entirely or partly to inefficient 3'-end formation. Our finding that the simultaneous deletion of introns 1 through 5 results in an abnormally high level of C^-/A^- transcripts and an abnormally low level of C^+/A^+ transcripts indicates that the presence of intron 6 is not sufficient for efficient 3'-end formation and is consistent with the idea that one or more of the other introns might also function in 3'-end formation (unpublished data). Additional ways in which the intron deletions could result in an abnormally low level of C^+/A^+ transcripts include but are not limited to (i) disruption of other posttranscriptional metabolic events that are distinct from splicing but coordinated by one or more of the introns and (ii) disruption of the RNA folding pathway.

The final intron might contain specific sequences that function more effectively in 3'-end formation than do the sequences of the upstream intron(s). In theory, these specific sequences could reside between the donor, lariat, and the acceptor splice sites or could consist of the splice sites themselves, or both. If spliceosome assembly on the last intron rather than the process of intron removal per se facilitates 3'-end formation, then these specific sequences could confer a rate of intron removal that is sufficiently slow relative to the rate of spliceosome assembly to provide sufficient time between the two processes for the commitment if not the completion of 3'-end formation. Alterna-

tively, the distance between the final intron and the pA site might influence 3′-end formation. If so, then the decrease in the efficiency of 3′-end formation as a consequence of deleting the last intron would be the result of an increase in this distance by the size of the penultimate exon. If the maintenance of a particular distance between the final intron and the pA site is a requirement for efficient 3′-end formation, then this distance must be quite variable between genes given the large variations in the size of last exons (22). Furthermore, it was demonstrated for the β-globin gene of *Xenopus laevis* that a reduction in the distance between the last intron and the pA site by 80 bp had no effect on either the efficiency or the accuracy of cleavage and polyadenylation (31).

Experiments planned for the future aim to define for TPI pre-mRNA the mechanism by which intron 6 sequences function in 3′-end formation and to determine if other introns other than intron 6 influence the efficiency of 3′-end formation.

ACKNOWLEDGMENTS

We thank Jodi Giancola O'Brien for excellent technical assistance, Alfred Cairo for oligonucleotide synthesis, Carl Porter for Malme-3 cells, members of our laboratory and John Yates for helpful discussions, and Nancy Frame for typing.

This work was supported by Public Health Service research grant DK 33938 from the National Institutes of Health and by the Council for Tobacco Research-U.S.A., Inc. (CTR grant 3341M).

REFERENCES

1. **Aviv, H., and P. Leder.** 1972. Purification of biologically active globin messenger RNA by chromatography on oligothymidylic acid-cellulose. Proc. Natl. Acad. Sci. USA **69:**1408–1412.
2. **Barrett, N. L., G. G. Carmichael, and Y. Luo.** 1991. Splice site requirement for the efficient accumulation of polyoma virus late mRNAs. Nucleic Acids Res. **19:**3011–3017.
3. **Birnstiel, M. L., M. Busslinger, and K. Strub.** 1985. Transcription termination and 3′ processing: the end is in site! Cell **41:**349–359.
4. **Boyer, T. G., J. R. Krug, and L. E. Maquat.** 1989. Transcriptional regulatory sequences of the housekeeping gene for human triosephosphate isomerase. J. Biol. Chem. **264:**5177–5187.
5. **Brinster, R. L., J. M. Allen, R. R. Behringer, R. E. Gelinas, and R. D. Palmiter.** 1988. Introns increase transcriptional efficiency in transgenic mice. Proc. Natl. Acad. Sci. USA **85:**836–840.
6. **Buchman, A. R., and P. Berg.** 1988. Comparison of intron-dependent and intron-independent gene expression. Mol. Cell. Biol. **8:**4395–4405.
7. **Callis, J., M. Fromm, and V. Walbot.** 1987. Introns increase gene expression in cultured maize cells. Genes Dev. **1:**1183–1200.
8. **Chang, D. D., and P. Sharp.** 1989. Regulation by HIV rev depends upon recognition of splice sites. Cell **59:**789–795.
9. **Chen, I.-T., and L. A. Chasin.** 1993. Direct selection for mutations affecting specific splice sites in a hamster dihydrofolate reductase minigene. Mol. Cell. Biol. **13:**289–300.
10. **Cheng, J., M. Fogel-Petrovic, and L. E. Maquat.** 1990. Translation to near the distal end of the penultimate exon is required for normal levels of spliced triosephosphate isomerase mRNA. Mol. Cell. Biol. **10:**5215–5225.
11. **Chiou, H. C., C. Dabrowski, and J. C. Alwine.** 1991. Simian virus 40 late mRNA leader sequences involved in augmenting mRNA accumulation via multiple mechanisms, including increased polyadenylation efficiency. J. Virol. **65:**6677–6685.
12. **Collis, P., M. Antoniou, and F. Grosveld.** 1990. Definition of the minimal requirements within the human β-globin gene and the dominant control region for high level expression. EMBO J. **9:**233–240.
13. **Daar, I. O., and L. E. Maquat.** 1988. Premature translation termination mediates triosephosphate isomerase mRNA degradation. Mol. Cell. Biol. **8:**802–813.
14. **Dreyfuss, G., M. S. Swanson, and S. Piñol-Roma.** 1988. Heterogeneous nuclear ribonucleoprotein particles and the pathway of mRNA formation. Trends Biochem. **13:**86–91.
15. **Eckner, R., W. Ellmeier, and M. L. Birnstiel.** 1991. Mature mRNA 3′ end formation stimulates RNA export from the nucleus. EMBO J. **10:**3513–3522.
16. **Fineberg, A. P., and B. Vogelstein.** 1983. A technique for radiolabeling DNA restriction endonuclease fragments to high specific activity. Anal. Biochem. **132:**6–13.
17. **Gasser, C. S., C. C. Simonsen, J. W. Schilling, and R. T. Schimke.** 1982. Expression of abbreviated mouse dihydrofolate reductase gene in cultured hamster cells. Proc. Natl. Acad. Sci. USA **79:**6522–6526.
18. **Green, M. R., and M. L. Zapp.** 1989. Revving up gene expression. Nature (London) **338:**200–201.
19. **Gruss, P., and G. Khoury.** 1980. Reserve of a splicing defective mutant by insertion of an heterologous intron. Nature **286:**634–637.
20. **Gruss, P., C.-J. Lai, R. Dhar, and G. Khoury.** 1979. Splicing as a requirement for biogenesis of functional 16S mRNA of simian virus 40. Proc. Natl. Acad. Sci. USA **76:**4317–4321.
21. **Hamer, D. H., K. D. Smith, S. H. Boyer, and P. Leder.** 1979. SV40 recombinants carrying rabbit β-globin gene coding sequences. Cell **17:**725–735.
22. **Hawkins, J. D.** 1988. A survey on intron and exon lengths. Nucleic Acids Res. **16:**9893–9908.
23. **Huang, M. T.-F., and C. M. Gorman.** 1990. Intervening sequences increase efficiency and accumulation of cytoplasmic RNA. Nucleic Acids Res. **18:**937–947.
24. **Kermekchiev, M., M. Pettersson, P. Matthias, and W. Schaffner.** 1991. Every enhancer works with every promoter for all the combinations tested: could new regulatory pathways evolve by enhancer shuffling? Gene Exp. **1:**71–81.
25. **Kopczynski, C. C., and M. A. T. Muskavitch.** 1992. Introns excised from the *delta* primary transcript are localized near sites of *delta* transcription. J. Cell Biol. **119:**503–512.
26. **Kunkel, T. A., J. D. Roberts, and R. A. Zakour.** 1987. Rapid and efficient site-specific mutagenesis without phenotype selection. Methods Enzymol. **154:**376–382.
27. **Lamond, A. I.** 1991. Nuclear RNA processing. Curr. Opin. Cell. Biol. **3:**493–501.
28. **Legrain, P., and M. Rosbash.** 1989. Some *cis* and *trans*-acting mutants for splicing target pre-mRNA to the cytoplasm. Cell **57:**573–583.
29. **Maniatis, T.** 1991. Mechanisms of alternative pre-mRNA splicing. Science **251:**33–34.
30. **Maquat, L. E., R. Chilcote, and P. M. Ryan.** 1985. Human triosephosphate isomerase cDNA and protein structure: studies of triosephosphate isomerase deficiency in man. J. Biol. Chem. **260:**3748–3753.
31. **Mason, P. J., J. A. Elkington, M. M. Lloyd, M. B. Jones, and J. G. Williams.** 1986. Mutations downstream of the polyadenylation site of a Xenopus β-globin mRNA affect the positions but not the efficiency of 3′ processing. Cell **46:**263–270.
32. **McKeown, M.** 1992. Alternative mRNA splicing. Annu. Rev. Cell Biol. **8:**133–155.
33. **McMaster, G. K., and G. G. Carmichael.** 1977. Analysis of single- and double-stranded nucleic acids on polyacrylamide and agarose gels by using glyoxal and acridine orange. Proc. Natl. Acad. Sci. USA **74:**4835–4838.
34. **Mitchell, P. J., and R. Tjian.** 1989. Transcriptional regulation in mammalian cells by sequence-specific DNA binding proteins. Science **244:**371–378.
35. **Neuberger, W. S., and G. T. Williams.** 1988. The intron requirement for immunoglobulin gene expression is dependent upon the promoter. Nucleic Acids Res. **16:**6713–6724.
36. **Niwa, M., and S. M. Berget.** 1991. Polyadenylation precedes splicing in vitro. Gene Expr. **1:**5–14.
37. **Niwa, M., and S. M. Berget.** 1991. Mutation of the AAUAAA polyadenylation signal depresses in vitro splicing of proximal but not distal introns. Genes Dev. **5:**2086–2095.

38. **Niwa, M., C. C. MacDonald, and S. M. Berget.** 1992. Are vertebrate exons scanned during splice-site selection? Nature (London) **360:**277–280.
39. **Niwa, M., S. D. Rose, and S. M. Berget.** 1990. In vitro polyadenylation is stimulated by the presence of an upstream intron. Genes Dev. **4:**1552–1559.
40. **Palmiter, R. D., E. P. Sandgren, M. R. Avarbock, D. D. Allen, and R. L. Brinster.** 1991. Heterologous introns can enhance expression of transgenes in mice. Proc. Natl. Acad. Sci. USA **88:**478–482.
41. **Pandey, N. B., N. Chodchoy, T.-J. Liu, and W. F. Marzluff.** 1990. Introns in histone genes alter the distribution of 3' ends. Nucleic Acids Res. **18:**3161–3170.
42. **Robberson, B. L., G. J. Cote, and S. M. Berget.** 1990. Exon definition may facilitate splice site selection in RNAs with multiple exons. Mol. Cell. Biol. **10:**84–94.
43. **Ryu, W.-S., and J. E. Mertz.** 1989. Simian virus 40 late transcripts lacking excisable intervening sequences are defective in both stability in the nucleus and transport to the cytoplasm. J. Virol. **63:**4386–4394.
44. **Sheets, D. M., C. S. Ogg, and M. P. Wickens.** 1990. Point mutations in AAUAAA and the poly(A) addition site effects on the accuracy and efficiency of cleavage and polyadenylation in vitro. Nucleic Acids Res. **18:**5799–5805.
45. **Smith, C. W. J., J. G. Patton, and B. Nadal-Ginard.** 1989. Alternative splicing in the control of gene expression. Annu. Rev. Genet. **23:**527–577.
46. **Stolow, D. T., and S. M. Berget.** 1990. UV cross-linking of polypeptides associated with 3'-terminal exons. Mol. Cell. Biol. **10:**5937–5944.
47. **Sveren, J., and R. Chalkley.** 1990. The structure and assembly of active chromatin. Trends Genet. **6:**52–56.
48. **Treisman, R., U. Novak, J. Favaloro, and R. Kamen.** 1981. Transformation of rat cells by an altered polyoma virus genome expressing only the middle-T protein. Nature (London) **292:** 595–600.
49. **Villarreal, L. P., and R. T. White.** 1983. A splice junction deletion deficient in the transport of RNA does not polyadenylate nuclear RNA. Mol. Cell. Biol. **3:**1381–1388.
50. **Wahle, E., and W. Keller.** 1992. The biochemistry of 3'-end cleavage and polyadenylation of messenger RNA precursors. Annu. Rev. Biochem. **61:**419–440.
51. **Wickens, M.** 1990. In the beginning is the end: regulation of poly(A) addition and removal during early development. Trends Biochem. Sci. **15:**320–324.
52. **Wickens, M.** 1990. How the messenger got its tail: addition of poly(A) in the nucleus. Trends Biochem. Sci. **15:**277–281.